FEBS
Letters

journal homepage: www.FEBSLetters.org

Review

Neuronal circuits and computations: Pattern decorrelation in the olfactory bulb

CrossMark

Rainer W. Friedrich [a,b,*], Martin T. Wiechert [c,d]

[a] *Friedrich Miescher Institute for Biomedical Research, Maulbeerstrasse 66, 4058 Basel, Switzerland*
[b] *University of Basel, 4003 Basel, Switzerland*
[c] *Laboratory for Perception and Memory, Institut Pasteur, 25 rue du Docteur Roux, 75724 Paris, France*
[d] *CNRS UMR3571, 25 rue du Docteur Roux, 75724 Paris, France*

ARTICLE INFO

ABSTRACT

Neuronal circuits in the olfactory bulb transform odor-evoked activity patterns across the input channels, the olfactory glomeruli, into distributed activity patterns across the output neurons, the mitral cells. One computation associated with this transformation is a decorrelation of activity patterns representing similar odors. Such a decorrelation has various benefits for the classification and storage of information by associative networks in higher brain areas. Experimental results from adult zebrafish show that pattern decorrelation involves a redistribution of activity across the population of mitral cells. These observations imply that pattern decorrelation cannot be explained by a global scaling mechanism but that it depends on interactions between distinct subsets of neurons in the network. This article reviews insights into the network mechanism underlying pattern decorrelation and discusses recent results that link pattern decorrelation in the olfactory bulb to odor discrimination behavior.

© 2014 Federation of European Biochemical Societies. Published by Elsevier B.V. All rights reserved.

1. Computational functions of neuronal circuits and the olfactory system

Higher brain functions are not directly determined by the biophysical properties of individual neurons but emerge from interactions between many neurons in synaptically connected networks. Deciphering such networks is central to understanding the principles of biological computation, the relationship between brains and computers, brain dysfunction in mental disorders, and the very nature of humans and other animals. Neurons are organized in structured networks, or circuits, that are typically defined as circumscribed populations of interconnected neurons. Small circuits such as repetitive columnar elements of the optic lobes in Drosophila may be comprised of <100 neurons [1] while large circuits such as mammalian piriform cortex or cerebellar lobules can contain 10^6 neurons or more [2]. Most neuronal circuits consist of functionally diverse types of neurons and contain prominent feedback loops. The computational potential of such systems is enormous [3] but we are only beginning to understand how this potential is realized in biological circuits. A systematic and somewhat reductionist approach to understand brain functions may thus ask *what* different circuits compute, and *how* these computations are achieved mechanistically as neurons exchange and integrate biophysical signals.

The challenge to understand a neuronal computation obviously depends on the complexity of the computation and the underlying circuit. Some computations can be described based on first-order statistical properties of neuronal connectivity (average connection strength) and based on univariate properties of neuronal activity or simply mean firing rate. These quantities can often be measured using well-established methods and the computations can often be described by tractable mathematical models. One example of such a computation is "normalization", an important elementary operation that scales responses of individual neurons as a function of the mean population activity [4,5]. Other computations, however, depend on higher-order properties of connectivity and on multivariate properties of activity patterns. These diverse and potentially complex computations have not yet been explored exhaustively. Some of these computations are likely to depend on the activity of specific subsets of neurons and on specific connectivity. For example, receptive field properties of neurons in primary visual cortex are thought to be shaped by specific

* Corresponding author at: Friedrich Miescher Institute for Biomedical Research, Maulbeerstrasse 66, 4058 Basel, Switzerland.
  E-mail address: Rainer.Friedrich@fmi.ch (R.W. Friedrich).

connectivity among neurons with similar feature selectivity [6], and storage of arbitrary information in memory networks such as the hippocampus is thought to depend on experience-dependent modifications of synaptic connections between specific subsets of neurons [7]. Analyzing the mechanisms underlying such computations, and even defining the computations themselves, is often hampered by experimental constraints. It is, for example, possible to record activity only from subsets of neurons within a large population. The sample size of population activity measurements may thus be sufficient to determine simple statistical properties of neuronal activity patterns but fail to resolve higher-order features. Detailed descriptions of the connectivity among individual neurons are lacking for most circuits, with few exceptions [1,8–10]. Furthermore, mathematical analyses of networks with higher-order structure can become extremely complex. Understanding neuronal computations depending on higher-order circuit features is therefore a major challenge in neuroscience.

This review focuses on the decorrelation of odor-evoked activity patterns in the OB, a computation that reduces the overlap (Pearson product-moment correlation coefficient) between activity patterns representing different, yet structurally similar, odors. A neuronal activity pattern at time t may be represented by a vector where each element represents the firing rate of one neuron, measured during a small time window around t. Highly overlapping activity patterns are thus represented by vectors that have a high Pearson correlation coefficient, i.e., they project in similar directions within the high-dimensional coding space. Pattern decorrelation reorganizes activity patterns so that the Pearson correlation coefficient of the corresponding activity vectors decreases and their angular separation increases. As a consequence, it becomes easier to find a procedure – a classifier – to distinguish between the activity vectors. Pattern decorrelation is thus useful for pattern classification, a key operation in many higher brain functions such as object recognition, decision making and associative memory. Models of pattern classification in the brain assume that activity patterns are at least partially decorrelated. This assumption is often necessary to achieve good performance, to avoid destructive phenomena such as catastrophic interference, and to enable various other operations [11–17]. However, few studies have directly analyzed pattern decorrelation in the brain, possibly because it has been difficult to measure neuronal activity patterns across large numbers of neurons.

One brain area where pattern decorrelation was observed is the dentate gyrus of the hippocampus [18,19], which is assumed to pre-process activity patterns representing complex, multisensory information for storage and classification in other hippocampal subfields such as CA3 [20,21]. However, the underlying mechanisms are not understood in detail. Another brain area where pattern decorrelation has been studied is the OB, particularly in zebrafish [22–26]. Among the multiple targets of the OB is the piriform cortex, a large paleocortical area with an architecture similar to that of hippocampal area CA3. Like CA3, piriform cortex has been proposed to function as an associative memory system for the storage of information encoded by distributed activity patterns [27–29]. Pattern decorrelation may therefore subserve similar general functions in the OB and in the dentate gyrus although differences in the neuronal architecture of these circuits suggest that the underlying mechanisms are not identical.

The OB is the only olfactory processing center between sensory neurons in the nose and multiple higher telencephalic areas. Olfactory input reaches the OB through an array of discrete input channels, the olfactory glomeruli (Fig. 1), each of which receives convergent input from sensory neurons expressing the same odorant receptor [30]. Individual odorant receptors and glomeruli respond to multiple odorants, and each odorant activates a specific combination of glomeruli [30,31] (Fig. 2A). Odors are therefore
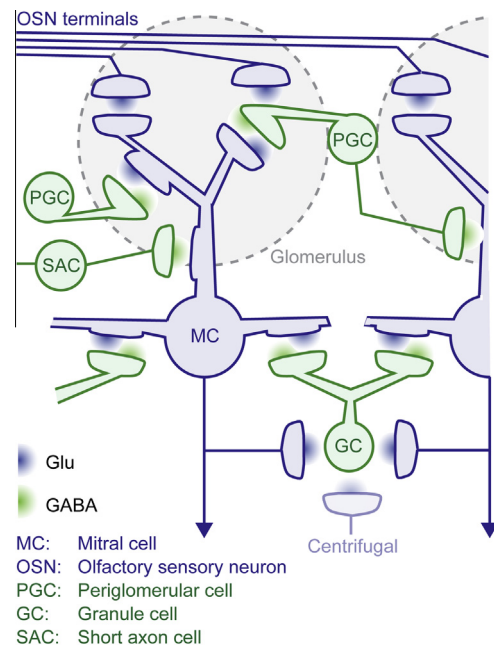

Fig. 1. Schematic illustration of selected cell types and synaptic connections in the OB. Modified from [91].

encoded in a combinatorial fashion and presented to the OB as discrete, usually distributed, glomerular activation patterns. Odorants with similar molecular features activate overlapping combinations of glomeruli, probably as a direct consequence of the molecular mechanisms governing receptor-ligand interactions. Glomerular representations of chemically similar odorants are therefore highly correlated. In order to facilitate stimulus classification, autoassociative memory and other tasks it appears useful to reduce these correlations at an early stage of sensory processing.

Sensory input from the array of glomeruli is processed in the OB by a network of principal neurons, the mitral/tufted cells (MCs), and multiple classes of interneurons including periglomerular cells, short-axon cells and granule cells [32] (Fig. 1). MCs are glutamatergic, receive glutamatergic input from sensory neurons and inhibitory input from interneurons, and convey the output of the OB to multiple higher brain areas including piriform cortex. Individual MCs receive sensory input only from one or a few glomeruli and are not directly coupled to MCs associated with other glomeruli. Periglomerular cells are located in the input (glomerular) layer of the OB and comprise multiple subtypes [33]. They are small neurons that receive input from various sources and provide GABAergic output to MCs. Short-axon cells are also located mainly in superficial layers but often have long processes [34]. They can have inhibitory or depolarizing effects on MCs that are mediated by GABAergic synapses and gap junctions, respectively [35]. Granule cells are located in deep layers and are by far the most numerous cell type in the OB. They are axonless, receive glutamatergic input from dendrites and axon collaterals of MCs, and make GABAergic synapses back onto MCs. Many of the dendro-dendritic connections between MCs and granule cells are reciprocal. The synaptic connectivity among neurons in the OB therefore provides multiple paths for interactions between MCs, even though MCs are not directly connected across glomeruli. These synaptic pathways extend over multiple spatial scales and often have inhibitory effects on MCs. In addition, multiple types of interneurons, but not MCs, receive input from higher brain areas.

MCs respond to odor stimulation with slow modulations of their firing rates (Fig. 2B) and with oscillatory synchronizations of action potentials in the beta and gamma frequency bands.

Similar observations have been made in a wide variety of species [36]. Moreover, complex population odor responses including firing rate modulations and oscillatory synchronization have also been observed in the antennal lobe, the first olfactory processing center of insects [36]. Combinatorial odor representations are therefore transformed at an early stage of olfactory processing but the associated computations have long remained obscure. Work in the OB of adult zebrafish revealed that one computation of the OB is a decorrelation of overlapping odor representations [22–25]. The adult zebrafish provides various experimental advantages for studying such circuit-level computations [37,38]. Importantly, the small size of the zebrafish brain allows for exhaustive measurements of neuronal activity patterns by multiphoton calcium imaging even in the adult and it offers unique opportunities for dense reconstructions of neuronal wiring diagrams [39].

2. Pattern decorrelation in the olfactory bulb

Odor-evoked inputs to the array of glomeruli can be measured optically after introducing calcium sensors selectively into olfactory sensory neurons [31,40–42]. In zebrafish, this method has been used to analyze glomerular activation patterns evoked by 16 amino acids at an intermediate concentration [31] (Fig. 2A). As these stimuli are natural odorants for many aquatic species, they define a biologically relevant stimulus subspace that comprises highly similar molecules (e.g., Phe/Tyr/Trp) as well as more dissimilar ones (e.g., basic vs. neutral amino acids).

Amino acids activated multiple glomeruli that were distributed, although not randomly, throughout a relatively large subregion of the OB [31,40]. In order to explore how glomerular inputs are processed within the OB, responses to the same set of amino acid stimuli were measured across the output neurons (MCs) by electrophysiological recordings or by temporally deconvolved multiphoton calcium imaging. The latter method uses optical measurements of somatic calcium signals to estimate neuronal firing rate changes, relative to baseline, across large populations of neurons [23–26,43–45]. Odor stimulation evoked different, odor-dependent firing rate changes in different MCs (Fig. 2B). Firing rates were often dynamically modulated during the first few hundred milliseconds of an odor response before they approached a steady state. Activity patterns were therefore analyzed using a sliding time window and represented by time series of activity vectors. Subsets of MCs rhythmically synchronized their action potentials with millisecond precision, giving rise to oscillatory population activity. This oscillatory synchronization emerged during the first few hundred milliseconds of the odor response, concomitant with the evolution of firing rates towards the steady state. The frequency of the oscillation was near 20 Hz and action potentials of different MCs were synchronized with near-zero phase lag [23]. Similar observations were made in a wide range of other species [36].

The evolution of MC activity patterns towards the steady state reflects processing within the OB because sensory inputs were almost static for the duration of stimulus presentation [24]. During this dynamic phase, firing rates of some MCs increased or decreased substantially but the mean firing rate across the population changed only slightly. Moreover, response profiles of MCs to different odorants changed during the dynamic phase but the mean tuning width remained almost constant [24]. Hence, OB output is not systematically broadened or sharpened as the steady state is approached but activity is redistributed across the MC population.

Shortly after response onset, amino acids that evoked highly correlated glomerular inputs also evoked highly correlated activity patterns across MCs. Subsequently, however, most of these output correlations decreased substantially (Fig. 2C). One computation associated with the reorganization of MC activity patterns is therefore a decorrelation of odor representations. This decorrelation is not simply caused by an increase in noise or by chaotic dynamics because trial-to-trial variability decreased, rather than increased, during an odor response. Hence, odor representations become not only more distinct but also more reliable as MC activity approaches the steady state [22–25].

The relationship between pattern decorrelation and oscillatory synchronization was analyzed by sorting individual MC action potentials into "synchronized" or "non-synchronized" subsets based on their phase relationship to the LFP oscillation [23]. Different odors caused synchronization among different ensembles of MCs. The majority of action potentials were, however, not strongly phase-locked ("non-synchronized"). Activity vectors constructed from the "non-synchronized" subset of action potentials showed pronounced decorrelation. Activity vectors constructed from the complementary subset of "synchronized" action potentials, in contrast, did not decorrelate [23]. When all action potentials were included in the activity vectors, activity vectors became decorrelated because the majority of action potentials were "non-synchronized". Hence, information about the original correlations is retained in the activity of "synchronized" MC subsets while the overall activity patterns undergo decorrelation. Decorrelated activity patterns are particularly informative about precise odor identity while the original correlations contain information about the "molecular category" of an odor. Precise identity and the molecular category are complementary stimulus properties because one reflects molecular differences whereas the other reflects common features. The OB therefore extracts information about complementary stimulus properties and transmits this information simultaneously to higher brain areas in a multiplexed fashion.

The time course of pattern decorrelation depended on the odor stimulus. On average, decorrelation of "non-synchronized" MC activity patterns reached a steady state approximately 400 ms after response onset [23]. In these experiments, the odor pulse was not a sharp step but increased gradually for approximately 400–600 ms before reaching a plateau [46]. Such slowly rising stimuli are likely to be physiologically relevant because the natural habitat of zebrafish are still or slowly flowing waters. When olfactory bulb input was activated rapidly by optogenetic stimulation of sensory neurons [47], a steady state was reached much faster. Faster odor stimuli are thus expected to cause a more rapid transition to the steady state but this hypothesis has not been tested directly.

In order to examine the spatial redistribution of neuronal activity during odor responses, odor-evoked activity across large numbers of neurons was measured by temporally deconvolved multiphoton calcium imaging [44,45,48]. MCs and interneurons were distinguished by genetically expressed fluorescent markers. During the early phase of odor responses, some MCs responding to odorants with similar molecular features were found to be spatially clustered in the vicinity of glomerular clusters with similar response profiles. The overlap of clustered MC activity accounted for much of the high pattern correlations during the initial odor response. As the response progressed, subsets of these MCs became less active or silent while the density of activity outside clusters increased slightly. Hence, activity patterns were "locally sparsened" so that clustered activity gradually disappeared. This local sparsening resulted in decorrelation because the identity of MCs that were silenced depended on precise odor identity [44]. Further results indicated that local sparsening was caused by the inhibition of odor-specific subsets of MCs [49]. Consistent with this notion, the activity of interneurons, especially granule cells, increased as activity patterns across MCs were reorganized [44].

A biologically useful mechanism for pattern decorrelation should be resilient against small differences in inputs that may reflect noise. To examine this possibility the molecular identity of an odor was varied in small steps by "morphing" one amino acid
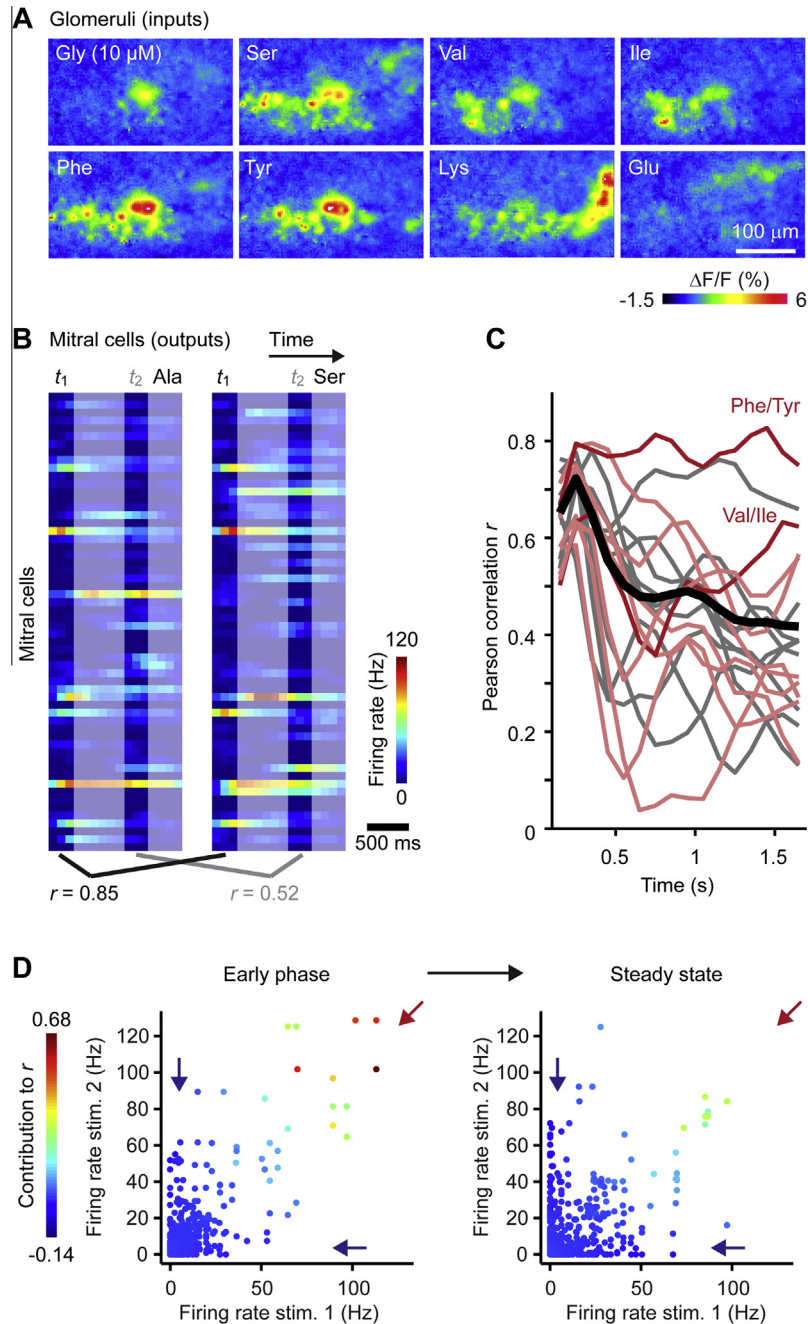
Fig. 2. Pattern decorrelation in the OB. (A) Glomerular activation patterns in the zebrafish OB evoked by 8 amino acid odorants (10 μM), measured by imaging of calcium signals in axon terminals from olfactory sensory neurons (modified from [31]). (B) Responses of 58 MCs to two similar amino acids (Ala, Ser; data from [23]). Color code represents firing rates of each neuron as a function of time. Shading depicts time windows at the beginning of the odor response (t_1) and during the steady state (t_2). r: Pearson correlation between activity patterns across the population of MCs during time windows t_1 and t_2. (C) Pairwise correlation between MC activity patterns evoked by amino acids as a function of time. Only pairs of patterns with high initial correlations (mean correlation 100–300 ms after response onset $\geqslant 0.6$) were included. Red lines correspond to odor pairs used in a behavioral discrimination task [86]. Fish failed to discriminate Phe/Tyr and Val/Ile (dark red lines). Gray lines correspond to odor pairs that were not tested in the behavioral task. Black line shows average. Modified from [22]. (D) Contribution of individual neurons to high pattern correlations during the early phase and during the steady state of the odor response. Each dot shows the response (firing rate) of one neuron to two stimuli and its contribution to the corresponding pairwise Pearson correlation between activity patterns across all neurons (color-code). Dots along the Cartesian axes indicate selective responses to one odor (blue arrows) while dots along the diagonal represent unselective responses to both odors (red arrow). The contribution of MC i to the pairwise Pearson correlation r is given by $(x_i - x_{mean})(y_i - y_{mean})/(s_x\, s_y)$ where x_i and y_i are responses of MC i to the two stimuli, x_{mean} and y_{mean} are the mean population responses, and s_x and s_y are the standard deviations. Only pairs of patterns with Pearson correlation $\geqslant 0.65$ during the early phase were included.

into another through a series of binary mixtures presented in pseudorandom sequence [26]. Steady-state MC activity patterns preserved input similarity within subranges of a morphing series but changed abruptly at defined transition points. Decorrelation therefore reflects a "discretization" of MC coding space into stable patches that are separated by instable transition regions. Abrupt

transitions between activity patterns were driven by coordinated response changes among small, odor-specific MC ensembles, rather than by global pattern changes [26].

How is the output of the OB interpreted in higher brain areas? We began to address this question by whole-cell patch clamp recordings and multiphoton calcium imaging in the posterior zone

of the dorsal telencephalon (Dp) of zebrafish. Dp is the largest target area of the OB in teleosts and directly homologous to mammalian olfactory (piriform) cortex [50]. Neurons often behave as "coincidence detectors" that respond more sensitively to synaptic input when it is synchronized with a precision in the range of milliseconds. The subset of synchronized action potentials within the MC population could thus have a strong impact on higher-order neurons and bias their responses to molecular categories. We therefore examined the sensitivity of Dp neurons to synchronized input by various approaches including optogenetic manipulations of oscillatory synchrony in the OB [47]. Dp neurons were found to be quite insensitive to synchrony and behaved as strong low-pass temporal filters, indicating that they act as "temporal integrators" rather than as coincidence detectors. Furthermore, most Dp neurons responded with action potentials during the steady-state of OB activity but not during the dynamic phase. Neuronal circuits in Dp therefore attenuate the impact of synchrony and appear to extract information mainly from the decorrelated steady states of MC activity. Hence, pattern decorrelation in the OB is likely to have direct consequences for odor representations in Dp.

3. Different forms of decorrelation

Before exploring the mechanisms underlying pattern decorrelation in the OB it is useful to consider some general issues related to decorrelation. Procedures for decorrelation may be adaptive or non-adaptive. Adaptive procedures are tuned to decorrelate inputs for which some prior knowledge exists. Such procedures include, for example, principal component analysis (PCA) and independent component analysis (ICA). These widely used methods project inputs onto orthogonal basis vectors that are defined based on an exemplary set of inputs. In the brain, adaptive decorrelation by a mechanism akin to ICA is, for example, found in visual cortex and in the early auditory system: receptive fields of neurons in these brain areas form a set of basis functions or filters that decorrelate responses of individual neurons to different natural images or sounds [51–53]. Obviously, the underlying receptive field properties have been optimized by evolution and/or experience to match the statistical properties of natural scenes or sounds. Other inputs may, however, not be decorrelated efficiently. Indeed, linear methods such as PCA and ICA will, on average, fail to decrease correlations among arbitrary sets of inputs [54]. Adaptive methods may therefore be powerful when statistical properties of inputs are predictable but perform poorly on non-predictable, arbitrary sets of inputs. Non-adaptive decorrelation procedures, in contrast, do not require prior knowledge and can decorrelate unpredictable inputs. In the brain, non-adaptive pattern decorrelation can be achieved by a convergent/divergent projection to a larger neuronal population and subsequent thresholding to create high-dimensional and sparse activity patterns. However, this strategy may be limited to large circuits such as the cerebellum, primary sensory cortices, or the insect mushroom body because it requires large numbers of neurons [14,36,52,54–56]. Generally, it is not well understood how non-adaptive decorrelation can be achieved by other mechanisms in smaller circuits.

It is also important to distinguish between pattern decorrelation and channel decorrelation. Pattern decorrelation concerns the pair-wise correlation between patterns across the different elements in a system, such as patterns of activity across neuronal populations (Fig. 3A). Channel decorrelation, in contrast, concerns the correlation between the channels of the system, such as pair-wise correlations between trains of action potentials of different neurons, or pair-wise correlations between the response profiles of different neurons to a set of stimuli (Fig. 3A). From a neurobiological perspective these operations are fundamentally different.

Channel decorrelation reduces the redundancy of information transmitted through different processing channels (neurons). This operation is central to "efficient coding", a framework that has been highly influential in neuroscience [57,58]. Moreover, channel decorrelation pertains to many problems in other disciplines; classical examples are source separation problems such as the unmixing of conversations in a "cocktail party" situation [59–62]. Channel decorrelation can, for example, be achieved by PCA and ICA. These methods produce decorrelated output channels by a linear combination (weighted sum) of input channels. In the context of a neural circuit, the weights may be directly interpreted as weights of synaptic interactions between neurons. Examples for channel decorrelation in the brain include the filtering of visual or auditory inputs by the receptive fields of neurons [51–53]. Generally, channel decorrelation is a widely studied operation that often has a direct neurobiological correlate.

Pattern decorrelation, in contrast, reduces the overlap between different patterns across channels (Fig. 3A), which occur at different times and, in the brain, usually encode distinct items. Pattern decorrelation therefore disambiguates representations of different items and facilitates the retrieval of information. The result of pattern decorrelation may thus be described as "informative coding" or "smart coding". Under special circumstances channel decorrelation can result in pattern decorrelation and vice versa but these computations can also occur separately (see [63] and references therein). The decorrelation of odor representations observed in the OB is a clear case of pattern decorrelation. It is not produced by increasing the dimensionality of coding space because activity across the same population of MCs is decorrelated over time. The OB is therefore an interesting model system to study mechanisms of pattern decorrelation in the brain.

4. Mechanisms of pattern decorrelation in the olfactory bulb

It has been proposed that the discriminability of activity patterns across MCs is increased by contrast enhancement through short-range lateral inhibition. This hypothesis was strongly influenced by image processing in the retina where spatial receptive fields with an excitatory center and an inhibitory surround are generated by lateral inhibition between neighboring, topographically organized processing channels [64]. The resulting local contrast enhancement is useful in vision because it emphasizes the representation of informative features in natural scenes (e.g., edges). A similar contrast enhancement was originally proposed to occur in the OB based on anatomical grounds and based on reports of MC receptive fields with a simple center-surround organization in "molecular space" [64–66]. However, subsequent studies failed to provide strong evidence for a simple topographic mapping of olfactory features onto the array of glomeruli [31,41,67] and for pronounced short-range lateral inhibition in the OB. Rather, a substantial fraction of inhibitory interactions appears to act over long distances [36,68–70]. Moreover, the hypothesis that short-range lateral inhibition optimizes odor representations has been challenged based on other arguments [70].

More recent work [71,72] proposed that the OB processes glomerular input patterns in a mostly channel-autonomous way, i.e., processing does not depend on the topography or on the fine structure of activity patterns. Rather, activity of each glomerulus is transformed separately and glomeruli interact only via global or very broad inhibition. Different models use different non-linear glomerular transfer functions referred to as "non-topographic contrast enhancement" [71] and "activity-dependent gating" [72]. It is, however, important to understand that contrast enhancement and pattern decorrelation are different computations that are not
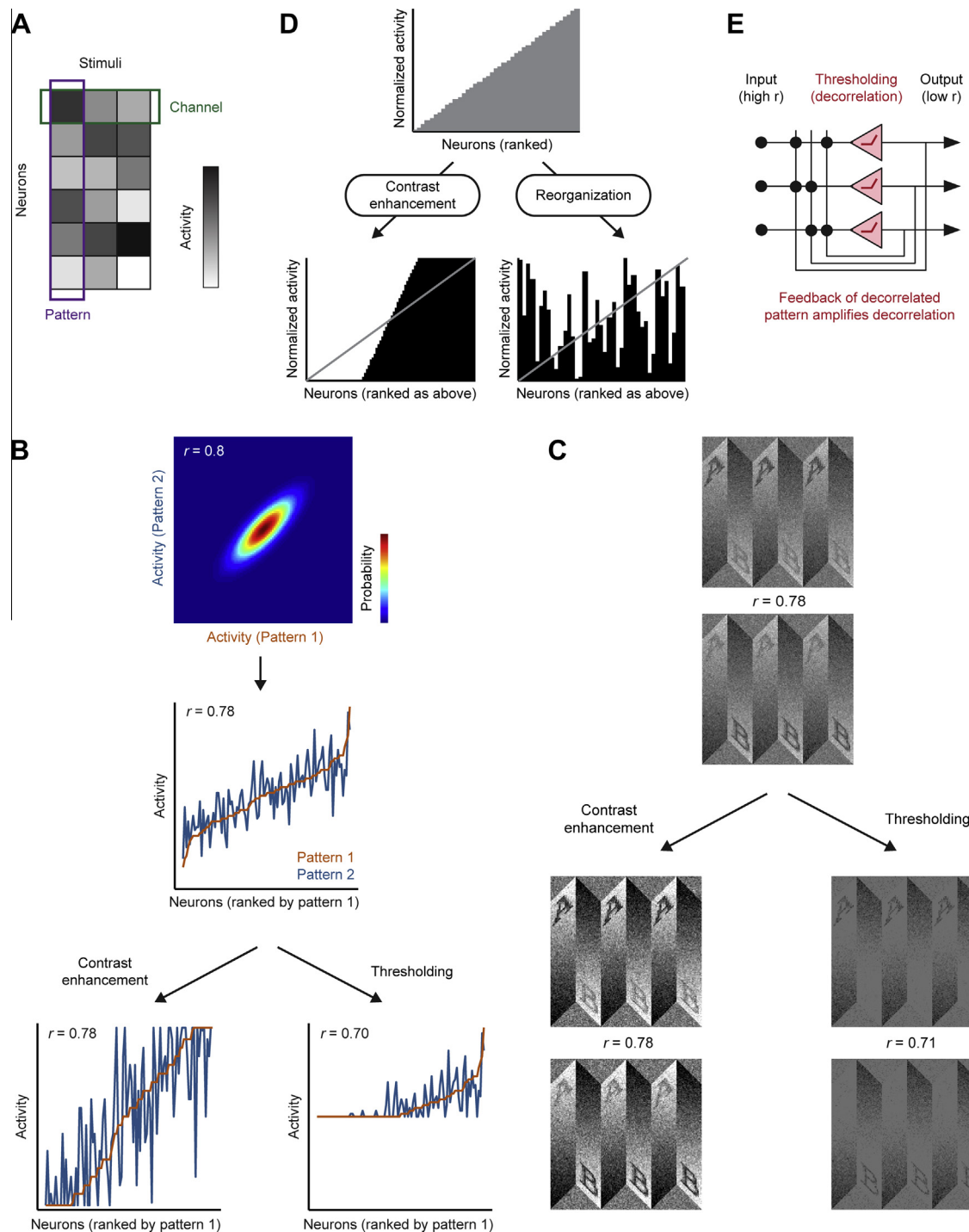
Fig. 3. Potential mechanisms of pattern decorrelation. (A) The arrangement of gray squares illustrates a typical data matrix representing responses of multiple neurons to multiple stimuli. "Channels" are neurons (rows) and "patterns" are responses of all neurons to a stimulus (columns). (B) Two patterns (top right) were drawn from a bivariate normal distribution with correlation $r = 0.8$ (top left). Bottom: transformation of the two patterns by global contrast enhancement (left) or thresholding (right), the initial step in reTIDe. The example illustrates that the pattern correlation r is decreased by thresholding but not by contrast enhancement. (C) Effects of contrast enhancement and thresholding on visual patterns. The example has been chosen to illustrate that decorrelation by thresholding can separate meaningful pattern components (letters A and B). Gray values in the original images are normally distributed. (D) Schematic illustration of contrast enhancement (left) and a more complex reorganization of activity patterns (right). Top (gray): hypothetical distribution of activity across a population of neurons. Bottom: activity distributions across the same population of neurons after transformations. (E) Schematic illustration of reTIDe by a SNORE (modified from [54]). An initial, possibly modest, decorrelation is produced by thresholding of an input pattern. This decorrelation is then amplified by combining the thresholded output with the input pattern via recurrent connections until the output approaches a steady state. Decorrelation is particularly pronounced when feedback connectivity is sparse and strong.

directly related. Linear contrast enhancement alone does not change the Pearson correlation. Consider, for example, pairs of patterns drawn from a correlated joint normal distribution. In the absence of substantial thresholding or other strong non-linearities,

contrast enhancement has minimal effects on their Pearson correlation (Fig. 3B and C). When input patterns are jointly normally distributed the notion of the "strength" of a non-linearity can be made precise in terms of the non-linearity's expansion into Hermite

polynomials (M.T.W. and R.W.F., unpublished observations). Some decorrelation may occur when contrast enhancement operations include more pronounced thresholding or other non-linear transformations, with precise effects depending on the specific non-linearity and the specific distribution (histogram) of input firing rates [71,72]. However, decorrelating effects may then be attributed more to the non-linear transformation than to contrast enhancement per se.

Although mostly channel-autonomous models can decorrelate some input patterns [72,73], various observations suggest that they cannot account for pattern decorrelation in the zebrafish OB. Importantly, these models fail to reproduce the observed redistribution of activity across the population of MCs. Moreover, in a 2D physical space, they do not reproduce local sparsening of strongly active MC clusters but rather have the opposite effect [72]. These observations indicate that pattern decorrelation in the OB cannot be explained by mostly channel-autonomous models but that it depends on the multivariate structure of odor-specific activity patterns (Fig. 3D).

In the zebrafish OB, high initial pair-wise pattern correlations included substantial contributions from MCs that responded strongly to both stimuli (Fig. 2D). Because both mostly channel-autonomous models tend to preserve high activity they would not be expected to efficiently decorrelate these activity patterns. As the odor response evolved, the activity of MCs then changed in a fashion that could not be predicted from their initial activity and the mean activity of the population (Fig. 2D). These results imply that input–output transforms of these MCs depend on multivariate features of the activity pattern. Mostly channel-autonomous models, however, do not consider any structure in the activity pattern beyond the global mean, and can therefore not reproduce this behavior. Hence, pattern decorrelation must involve neuron-to-neuron interactions that cannot be captured by a first-order statistical description of the circuit architecture.

The effect of non-topographic contrast enhancement on odor-evoked activity patterns was further examined by pharmacological experiments using dopamine [74]. Global application of dopamine hyperpolarized MCs and often increased their excitability so that responses to weak inputs were reduced while responses to strong inputs were affected only slightly. As a result, the contrast of odor-evoked MC activity patterns was enhanced approximately twofold in the presence of dopamine. Correlations between activity patterns were, however, not decreased [74]. These experimental results therefore support the notion that global contrast enhancement cannot account for pattern decorrelation in the zebrafish OB. Nevertheless, contrast enhancement may occur in the OB and subserve other functions as it is likely to influence neuronal responses in target areas of the OB.

New insights into pattern decorrelation came from the analysis of generic networks referred to as "stochastically connected networks of rectifying elements" (SNOREs; Fig. 3E) [54]. Neurons were modeled as threshold-linear units and recurrently connected with a given probability by a fixed weight. Because SNOREs allow for convergent and divergent interactions between neurons, each neuron's activity can be directly influenced by the activity of specific subsets of other neurons, and all neurons can indirectly influence each other. SNOREs can therefore produce input–output transforms that depend on multivariate features of neuronal activity patterns and differ from those of mostly channel-autonomous models.

Theoretical analyses and computational modeling demonstrated that large SNOREs decorrelate any set of positively correlated, normally distributed input patterns by a mechanism referred to as "recurrence-enhanced threshold-induced decorrelation" (reTIDe) [54]. The initial step is a thresholding of the input, i.e., an elementary non-linear operation that models the fact that

firing rates must be non-negative. Thresholding alone decreases correlations [14,54,75] (Fig. 3B and C), an effect that may also contribute to the decorrelation observed in mostly channel-autonomous models. In purely feed-forward systems, substantial decorrelation by this mechanism requires high thresholds and, thus, large numbers of neurons. In feedback circuits, however, the thresholded output is transmitted back into the network and further decorrelated until a steady state is reached. Recurrent connectivity therefore amplifies the initial decorrelation so that substantial pattern decorrelation can be achieved with lower thresholds and fewer neurons (Fig. 3E). This mechanism is non-adaptive and performs true pattern decorrelation. The decorrelation is most pronounced when input correlations are in the intermediate range but vanishes as the similarity between input patterns approaches identity. Hence, the computation is robust against small fluctuations that may represent noise. Biologically plausible pattern decorrelation therefore emerges naturally in non-linear recurrent neuronal circuits.

Pattern decorrelation by reTIDe is particularly pronounced when connectivity is sparse and when the baseline activity of neurons is high [54]. These are two characteristics of the OB whose function had remained elusive. reTIDe in the OB was thus explored in computer simulations of the zebrafish OB that included various features of the biological circuit such as realistic arrangements of glomeruli, a distance-dependent decay of connection probability, and symmetric inhibition between MCs [54]. Input patterns were derived from measured glomerular activation patterns. The simulated OB decorrelated overlapping inputs and reproduced a wide range of other experimental observations. Most of the observed decorrelation could be attributed to reTIDe. These results suggest that reTIDe is the primary mechanism underlying pattern decorrelation in the OB [54].

Generic reTIDe theory cannot explain why gradual morphing of one odor into another resulted in sudden transitions of MC activity patterns [26]. Nevertheless, there are multiple reasons why such transitions could occur in a biological system based on reTIDe. First, reTIDe theory has been developed for very large networks. Sudden transitions may thus arise as a consequence of small network size [76]. Second, step-like but non-conspicuous transitions may already be present in the input patterns (M.T.W and R.F., unpublished observations). ReTIDe would be expected to amplify these transitions if they fall within a certain range of input correlations [54]. Third, reTIDe theory assumes stochastic connectivity which is unlikely to be true for the OB [77] and most other circuits. Abrupt transitions between output patterns may thus be produced by biased interactions among subsets of neurons. Conceivably, biased connectivity could be introduced into a circuit by innate or experience-dependent mechanisms to enhance the decorrelation of specific odor representations. Deviations from stochastic connectivity could thus modify pattern decorrelation by reTIDe in an adaptive fashion without a fundamental change of the general mechanism.

Because reTIDe is non-adaptive it can decorrelate arbitrary normally distributed and other input patterns without prior knowledge. This property may be useful in olfaction since glomerular activation patterns experienced by an animal over its lifetime appear to be poorly predictable.

5. Functional roles of pattern decorrelation for information processing and behavior

Pattern decorrelation in the OB could obviously affect the discrimination of similar odors but this hypothesis is not trivial to examine. In has been proposed that some insights could be obtained by comparing the time course of pattern decorrelation to reaction

times in behavioral odor discrimination tasks. However, such an approach is problematic for various reasons. Some of these reasons concern technical issues such as the difficulty to measure behavioral reaction times in zebrafish, the slow onset of odor stimuli, and the fact that reaction times cannot be compared easily between species [22,78]. Other problems, however, are more fundamental. For example, a classifier designed to discriminate decorrelated steady states can already discriminate transient activity patters during the dynamical phase with good performance [26]. Steady states can thus be useful stable templates to learn classifiers for transient activity patterns early in the response. Fast behavioral reaction times are therefore not inconsistent with a function of steady states in the learning process. Moreover, it is important to consider that training of an animal in a discrimination task changes, and presumably optimizes, odor representations [79–82]. Hence, care must be taken in interpreting reaction times in a specific experimental paradigm as constraints for neuronal computations.

It has been frequently hypothesized that pattern decorrelation should be reflected in a behavioral speed-accuracy tradeoff because more decorrelated representations at later times should allow for more accurate discrimination. Such a speed-accuracy tradeoff has indeed been observed in rodents [83–85]. However, these observations could also be explained by other processing strategies such as temporal integration. In fact, the trial-to-trial variability (coefficient of variation) of MC odor responses decreases as the response approaches the steady state. Odor representations do therefore not only evolve towards increasingly distinct states but also accumulate information over time by other mechanisms. Reaction time measurements are therefore consistent with a function of pattern decorrelation in odor discrimination but do not provide conclusive evidence by themselves.

As a consequence of the data processing inequality, decorrelation per se does not increase the information content of activity patterns and, thus, cannot improve pattern classification by an optimal classifier (ideal observer). However, it can improve the performance of suboptimal classifiers and it can facilitate the process of finding some classifier with an acceptable tolerance range [22]. Pattern classification may thus have multiple benefits. For example, it may enable the use of pattern classification strategies that are suboptimal for highly correlated inputs but otherwise advantageous. Furthermore, it may decrease the time and effort it takes to learn new classifiers. Moreover, decorrelated representations can be more tolerant to noise arising at later stages of processing.

As a consequence of these benefits, pattern decorrelation may permit the brain to use simple classification strategies. Hence, the investment into decorrelation may reduce the overall overhead for information processing and allow for faster learning of classifiers. Decorrelation appears particularly important for pattern classification by attractor-like networks and associative memory. A central function of these operations is to map input patterns representing different items onto separate output patterns (pattern separation) but to converge inputs representing noisy or incomplete versions of the same item onto a common output pattern (pattern completion). High correlations between patterns representing different items may thus lead to incorrect pattern completion. Moreover, high correlations increase the risk of a destructive phenomenon known as catastrophic interference [13]. Models of associative memory and related pattern classification procedures thus assume that input patterns are at least partially decorrelated [11,12,16,17,21].

These considerations suggest two hypotheses that may be addressed to study potential reflections of pattern decorrelation in behavior. First, representations of odors that cannot be discriminated may remain highly correlated during an odor response. This hypothesis is based on the assumption that associative memory networks or related classification strategies may be unable to distinguish highly correlated inputs. Second, more efficient decorrelation of odor representations may be reflected by faster learning in a discrimination task. This hypothesis is based on the assumption that pattern decorrelation enables faster learning of new classifiers. Importantly, detailed measurements of pattern decorrelation are required to test both of these hypotheses.

The first hypothesis has been addressed in adult zebrafish. Miklavc and Valentinčič [86] used an associative conditioning task to examine odor discrimination between 62 pairs of amino acids. Correlations between the corresponding activity patterns had been determined in previous experiments [23–25]. Fish failed to discriminate only two of the 62 odor pairs, Phe/Tyr and Val/Ile. Initial correlations between the corresponding activity patterns were high but not substantially different from correlations between various other activity patterns. After the reorganization of activity patterns, however, correlations between the representations of Phe/Tyr and Val/Ile remained high while other correlations decreased (Fig. 2C). Furthermore, a specific zebrafish strain that decorrelated activity patterns evoked by Phe/Tyr also discriminated these odors in the behavioral test (Valentincic, unpublished observations; see [22]). These results are consistent with the first hypothesis that pattern decorrelation affects the ability to discriminate similar odor pairs.

Results pertaining to the second hypothesis have been obtained in mice. Behavioral experiments showed that more trials are needed to reach asymptotic performance in a discrimination task when the similarity of odor pairs is increased [84]. More recently, Gschwend, Carleton and colleages directly measured the decorrelation of various odor-evoked activity patterns in the OB and trained mice to discriminate the same odorants in a behavioral task. The rate of learning during the early phase of training could be predicted quantitatively from the amount of pattern decorrelation observed in the OB. These results strongly support the second hypothesis that pattern decorrelation increases the rate of discrimination learning.

Another approach to examine whether pattern decorrelation affects higher olfactory processing is to examine how neurons in higher brain areas decode patterns of MC activity. As mentioned above, Dp neurons appear to be tuned to those components of MC output patterns that are decorrelated and particularly informative about precise odor identity. Consistent with this observation, odor-evoked activity patterns in Dp were not highly correlated, even in response to similar amino acids [47,48]. These results indicate that pattern decorrelation in the OB shapes odor representations in higher brain areas.

6. Conclusions and outlook

Pattern decorrelation is a useful computation for pattern classification, an operation that is at the core of various higher brain functions. Experiments in the olfactory system have characterized pattern decorrelation in some detail, provided insights into the underlying circuit mechanisms, and indicate that this computation influences information processing in higher brain areas and behavior. Pattern decorrelation in the OB is a computation that depends on multivariate features of neuronal activity and higher-order features of connectivity [26,54]. Experimental and theoretical analyses of this computation have been greatly facilitated by exploiting advantages of adult zebrafish as an experimental model [38,39].

Our results suggest that pattern decorrelation is one of the primary functions of the OB. Another important computation in the OB is pattern equalization [35]. This computation is closely related to normalization and similar to computations in the insect

antennal lobe [87]. It stabilizes both the mean and the distribution of neuronal activity against variations in stimulus intensity. Together, decorrelation and equalization create distinct and partially concentration-invariant representations of different odors that are well-suited for discrimination by simple classifiers and associative networks. We therefore propose that a main function of the OB is to reformat odor representations for efficient pattern classification, which may be performed in various higher brain areas.

A separation of odor representations has also been observed in mice (Gschwend, Carleton and colleagues; unpublished observations) and in the antennal lobe of insects [88]. In the antennal lobe of locusts, odor representations are separated most efficiently during the dynamic phase rather than in the steady state [88]. The reason and functional significance of this species difference is currently unclear. One possibility is that the olfactory system of locusts is specialized to process transient odor representations because natural odor stimuli are usually short-lived. Moreover, computations in the antennal lobe and in the OB may not be identical because odor representations are decoded differently in higher brain areas of insects and vertebrates.

Several lines of evidence indicate that pattern decorrelation in the OB is achieved by a mechanism closely related to reTIDe, which relies on sparse feedback. The most obvious candidate pathway for this feedback is through granule cells, a large population of interneurons that are sparsely connected to MCs [77,89]. It would thus be interesting to analyze the precise architecture of MC–granule cell networks in more detail to quantify connection sparseness, to identify deviations from stochastic connectivity such as over-represented "circuit motifs", and to examine whether connectivity between neurons is related to their tuning properties. In general, the analysis of computations that depend on higher-order features of connectivity will be greatly facilitated if these connectivity features can be measured directly. This ambitious goal may now be addressed through exhaustive reconstructions of neuronal wiring diagrams by three-dimensional electron microscopy approaches [1,9,10,39,90], ideally in combination with measurements and manipulations of neuronal activity patterns.

Acknowledgements

References

[1] Takemura, S.Y. et al. (2013) A visual motion detection circuit suggested by Drosophila connectomics. Nature 500, 175–181.

[2] Shepherd, G.M. (2004) The Synaptic Organization of the Brain, Oxford University Press, New York.

[3] Maass, W., Joshi, P. and Sontag, E.D. (2007) Computational aspects of feedback in neural circuits. PLoS Comput. Biol. 3, e165.

[4] Heeger, D.J. (1992) Normalization of cell responses in cat striate cortex. Vis. Neurosci. 9, 181–197.

[5] Carandini, M. and Heeger, D.J. (2011) Normalization as a canonical neural computation. Nat. Rev. Neurosci. 13, 51–62.

[6] Harris, K.D. and Mrsic-Flogel, T.D. (2013) Cortical connectivity and sensory coding. Nature 503, 51–58.

[7] McNaughton, B.L. and Morris, R.G.M. (1987) Hippocampal synaptic enhancement and information storage within a distributed memory system. Trends Neurosci. 10, 408–415.

[8] White, J.G., Southgate, E., Thomson, J.N. and Brenner, S. (1986) The structure of the nervous system of the nematode Caenorhabditis elegans. Philos. Trans. R. Soc. London B Biol. Sci. 314, 1–340.

[9] Briggman, K.L., Helmstaedter, M. and Denk, W. (2011) Wiring specificity in the direction-selectivity circuit of the retina. Nature 471, 183–188.

[10] Helmstaedter, M., Briggman, K.L., Turaga, S.C., Jain, V., Seung, H.S. and Denk, W. (2013) Connectomic reconstruction of the inner plexiform layer in the mouse retina. Nature 500, 168–174.

[11] Hopfield, J.J. (1982) Neural networks and physical systems with emergent collective computational abilities. Proc. Natl. Acad. Sci. USA 79, 2554–2558.

[12] Itskov, V. and Abbott, L.F. (2008) Pattern capacity of a perceptron for sparse discrimination. Phys. Rev. Lett. 101, 018101.

[13] French, R.M. (1999) Catastrophic forgetting in connectionist networks. Trends Cogn. Sci. 3, 128–135.

[14] Marr, D. (1969) A theory of cerebellar cortex. J. Physiol. 202, 437–470.

[15] Kanerva, P. (1988) Sparse Distributed Memory, MIT Press, Cambridge, MA.

[16] Marr, D. (1970) A theory for cerebral neocortex. Proc. R. Soc. London B Biol. Sci. 176, 161–234.

[17] Kohonen, T. (1984) Self-organization and Associative Memory, Springer, Berlin.

[18] Leutgeb, J.K., Leutgeb, S., Moser, M.B. and Moser, E.I. (2007) Pattern separation in the dentate gyrus and CA3 of the hippocampus. Science 315, 961–966.

[19] McHugh, T.J. et al. (2007) Dentate gyrus NMDA receptors mediate rapid pattern separation in the hippocampal network. Science 317, 94–99.

[20] Rolls, E.T. and Kesner, R.P. (2006) A computational theory of hippocampal function, and empirical tests of the theory. Prog. Neurobiol. 79, 1–48.

[21] Treves, A., Tashiro, A., Witter, M.E. and Moser, E.I. (2008) What is the mammalian dentate gyrus good for? Neuroscience 154, 1155–1172.

[22] Friedrich, R.W. (2013) Information processing in the olfactory system of zebrafish. Annu. Rev. Neurosci. 36, 383–402.

[23] Friedrich, R.W., Habermann, C.J. and Laurent, G. (2004) Multiplexing using synchrony in the zebrafish olfactory bulb. Nat. Neurosci. 7, 862–871.

[24] Friedrich, R.W. and Laurent, G. (2001) Dynamic optimization of odor representations in the olfactory bulb by slow temporal patterning of mitral cell activity. Science 291, 889–894.

[25] Friedrich, R.W. and Laurent, G. (2004) Dynamics of olfactory bulb input and output activity during odor stimulation in zebrafish. J. Neurophysiol. 91, 2658–2669.

[26] Niessing, J. and Friedrich, R.W. (2010) Olfactory pattern classification by discrete neuronal network states. Nature 465, 47–52.

[27] Wilson, D.A. and Sullivan, R.M. (2011) Cortical processing of odor objects. Neuron 72, 506–519.

[28] Haberly, L.B. (2001) Parallel-distributed processing in olfactory cortex: new insights from morphological and physiological analysis of neuronal circuitry. Chem. Senses 26, 551–576.

[29] Hasselmo, M.E., Wilson, M.A., Anderson, B.P. and Bower, J.M. (1990) Associative memory function in piriform (olfactory) cortex: computational modeling and neuropharmacology. Cold Spring Harb. Symp. Quant. Biol. 55, 599–610.

[30] Buck, L.B. (2000) The molecular architecture of odor and pheromone sensing in mammals. Cell 100, 611–618.

[31] Friedrich, R.W. and Korsching, S.I. (1997) Combinatorial and chemotopic odorant coding in the zebrafish olfactory bulb visualized by optical imaging. Neuron 18, 737–752.

[32] Shepherd, G.M., Chen, W.R. and Greer, C.A. (2004) Olfactory bulb in: The Synaptic Organization of the Brain (Shepherd, G.M., Ed.), pp. 165–216, Oxford University Press, Oxford.

[33] Kosaka, K. and Kosaka, T. (2005) Synaptic organization of the glomerulus in the main olfactory bulb: compartments of the glomerulus and heterogeneity of the periglomerular cells. Anat. Sci. Int. 80, 80–90.

[34] Kiyokage, E. et al. (2010) Molecular identity of periglomerular and short axon cells. J. Neurosci. 30, 1185–1196.

[35] Zhu, P., Frank, T. and Friedrich, R.W. (2013) Equalization of odor representations by a network of electrically coupled inhibitory interneurons. Nat. Neurosci. 16, 1678–1686.

[36] Laurent, G. (2002) Olfactory network dynamics and the coding of multidimensional signals. Nat. Rev. Neurosci. 3, 884–895.

[37] Zhu, P., Fajardo, O., Shum, J., Zhang Schärer, Y.-P. and Friedrich, R.W. (2012) High-resolution optical control of spatiotemporal neuronal activity patterns in zebrafish using a digital micromirror device. Nat. Protoc. 7, 1410–1425.

[38] Friedrich, R.W., Jacobson, G.A. and Zhu, P. (2010) Circuit neuroscience in zebrafish. Curr. Biol. 20, R371–R381.

[39] Friedrich, R.W., Genoud, C. and Wanner, A.A. (2013) Analyzing the structure and function of neuronal circuits in zebrafish. Front. Neural Circuits 7, 71.

[40] Friedrich, R.W. and Korsching, S.I. (1998) Chemotopic, combinatorial and non-combinatorial odorant representations in the olfactory bulb revealed using a voltage-sensitive axon tracer. J. Neurosci. 18, 9977–9988.

[41] Wachowiak, M. and Cohen, L.B. (2001) Representation of odorants by receptor neuron input to the mouse olfactory bulb. Neuron 32, 723–735.

[42] Spors, H., Wachowiak, M., Cohen, L.B. and Friedrich, R.W. (2006) Temporal dynamics and latency patterns of receptor neuron input to the olfactory bulb. J. Neurosci. 26, 1247–1259.

[43] Friedrich, R.W., Yaksi, E., Judkewitz, B. and Wiechert, M.T. (2009) Processing of odor representations by neuronal circuits in the olfactory bulb. Ann. NY Acad. Sci. 1170, 293–297.

[44] Yaksi, E., Judkewitz, B. and Friedrich, R.W. (2007) Topological reorganization of odor representations in the olfactory bulb. PLoS Biol. 5, e178.

[45] Yaksi, E. and Friedrich, R.W. (2006) Reconstruction of firing rate changes across neuronal populations by temporally deconvolved Ca^{2+} imaging. Nat. Methods 3, 377–383.

[46] Tabor, R., Yaksi, E., Weislogel, J.M. and Friedrich, R.W. (2004) Processing of odor mixtures in the zebrafish olfactory bulb. J. Neurosci. 24, 6611–6620.

[47] Blumhagen, F., Zhu, P., Shum, J., Zhang Schärer, Y.-P., Yaksi, E., Deisseroth, K. and Friedrich, R.W. (2011) Neuronal filtering of multiplexed odour representations. Nature 479, 493–498.
[48] Yaksi, E., von Saint Paul, F., Niessing, J., Bundschuh, S.T. and Friedrich, R.W. (2009) Transformation of odor representations in target areas of the olfactory bulb. Nat. Neurosci. 12, 474–482.
[49] Tabor, R., Yaksi, E. and Friedrich, R.W. (2008) Multiple functions of GABA(A) and GABA(B) receptors during pattern processing in the zebrafish olfactory bulb. Eur. J. Neurosci. 28, 117–127.
[50] Mueller, T., Dong, Z., Berberoglu, M.A. and Guo, S. (2011) The dorsal pallium in zebrafish, Danio rerio (Cyprinidae, Teleostei). Brain Res. 1381, 95–105.
[51] Lewicki, M.S. (2002) Efficient coding of natural sounds. Nat. Neurosci. 5, 356–363.
[52] Olshausen, B.A. and Field, D.J. (1996) Emergence of simple-cell receptive field properties by learning a sparse code for natural images. Nature 381, 607–609.
[53] Bell, A.J. and Sejnowski, T.J. (1997) The "independent components" of natural scenes are edge filters. Vision Res. 37, 3327–3338.
[54] Wiechert, M.T., Judkewitz, B., Riecke, H. and Friedrich, R.W. (2010) Mechanisms of pattern decorrelation by recurrent neuronal circuits. Nat. Neurosci. 13, 1003–1010.
[55] Vinje, W.E. and Gallant, J.L. (2000) Sparse coding and decorrelation in primary visual cortex during natural vision. Science 287, 1273–1276.
[56] Perez-Orive, J., Mazor, O., Turner, G.C., Cassenaer, S., Wilson, R.I. and Laurent, G. (2002) Oscillations and sparsening of odor representations in the mushroom body. Science 297, 359–365.
[57] Barlow, H.B. (1961) Possible principles underlying the transformations of sensory messages in: Sensory Communication (Rosenblith, W.A., Ed.), pp. 217–234, MIT Press, Cambridge, MA.
[58] Barlow, H. (2001) Redundancy reduction revisited. Network 12, 241–253.
[59] S. Amari, A. Cichocki, H.H. Yang, Recurrent neural networks for blind separation of sources, in: International Symposium on Non-linear Theory and its Applications, NOLTA'95, Las Vegas, 1995, pp. 37–42.
[60] Weinstein, E., Feder, M. and Oppenheim, A.V. (1993) Multi-channel signal separation by decorrelation. IEEE Trans. Speech Audio Process. 1, 405–413.
[61] Brown, G.D., Yamada, S. and Sejnowski, T.J. (2001) Independent component analysis at the neural cocktail party. Trends Neurosci. 24, 54–63.
[62] Parra, L.C. and Spence, C.D. (2001) Separation of non-stationary natural signals in: Independent Component Analysis: Principles and Practice (Roberts, S. and Everson, R., Eds.), pp. 135–157, Cambridge University Press, Cambridge, MA.
[63] Wick, S.D., Wiechert, M.T., Friedrich, R.W. and Riecke, H. (2010) Pattern orthogonalization via channel decorrelation by adaptive networks. J. Comput. Neurosci. 28, 29–45.
[64] DeVries, S.H. and Baylor, D.A. (1993) Synaptic circuitry of the retina and olfactory bulb. Cell 72 (Suppl), 139–149.
[65] Yokoi, M., Mori, K. and Nakanishi, S. (1995) Refinement of odor molecule tuning by dendrodendritic synaptic inhibition in the olfactory bulb. Proc. Natl. Acad. Sci. USA 92, 3371–3375.
[66] Mori, K. and Shepherd, G.M. (1994) Emerging principles of molecular signal processing by mitral/tufted cells in the olfactory bulb. Stem Cell Biol. 5, 65–74.
[67] Soucy, E.R., Albeanu, D.F., Fantana, A.L., Murthy, V.N. and Meister, M. (2009) Precision and diversity in an odor map on the olfactory bulb. Nat. Neurosci. 12, 210–220.
[68] Fantana, A.L., Soucy, E.R. and Meister, M. (2008) Rat olfactory bulb mitral cells receive sparse glomerular inputs. Neuron 59, 802–814.
[69] Wachowiak, M. and Shipley, M.T. (2006) Coding and synaptic processing of sensory information in the glomerular layer of the olfactory bulb. Semin. Cell Dev. Biol. 17, 411–423.
[70] Laurent, G. (1999) A systems perspective on early olfactory coding. Science 286, 723–728.
[71] Cleland, T.A. and Sethupathy, P. (2006) Non-topographical contrast enhancement in the olfactory bulb. BMC Neurosci. 7, 7.
[72] Arevian, A.C., Kapoor, V. and Urban, N.N. (2008) Activity-dependent gating of lateral inhibition in the mouse olfactory bulb. Nat. Neurosci. 11, 80–87.
[73] Cleland, T.A., Johnson, B.A., Leon, M. and Linster, C. (2007) Relational representation in the olfactory system. Proc. Natl. Acad. Sci. USA 104, 1953–1958.
[74] Bundschuh, S.T., Zhu, P., Zhang Schärer, Y.-P. and Friedrich, R.W. (2012) Dopaminergic modulation of mitral cells and odor responses in the zebrafish olfactory bulb. J. Neurosci. 32, 6830–6840.
[75] de la Rocha, J., Doiron, B., Shea-Brown, E., Josic, K. and Reyes, A. (2007) Correlation between neural spike trains increases with firing rate. Nature 448, 802–806.
[76] Hahnloser, R.H., Seung, H.S. and Slotine, J.J. (2003) Permitted and forbidden sets in symmetric threshold-linear networks. Neural Comput. 15, 621–638.
[77] Willhite, D.C., Nguyen, K.T., Masurkar, A.V., Greer, C.A., Shepherd, G.M. and Chen, W.R. (2006) Viral tracing identifies distributed columnar organization in the olfactory bulb. Proc. Natl. Acad. Sci. USA 103, 12592–12597.
[78] Friedrich, R.W. (2006) Mechanisms of odor discrimination: neurophysiological and behavioral approaches. Trends Neurosci. 29, 40–47.
[79] Chapuis, J. and Wilson, D.A. (2011) Bidirectional plasticity of cortical pattern recognition and behavioral sensory acuity. Nat. Neurosci. 15, 155–161.
[80] Gottfried, J.A. (2009) Function follows form: ecological constraints on odor codes and olfactory percepts. Curr. Opin. Neurobiol. 19, 422–429.
[81] Rabin, M.D. (1988) Experience facilitates olfactory quality discrimination. Percept. Psychophys. 44, 532–540.
[82] Li, W., Howard, J.D., Parrish, T.B. and Gottfried, J.A. (2008) Aversive learning enhances perceptual and cortical discrimination of indiscriminable odor cues. Science 319, 1842–1845.
[83] Uchida, N. and Mainen, Z.F. (2003) Speed and accuracy of olfactory discrimination in the rat. Nat. Neurosci. 6, 1224–1229.
[84] Abraham, N.M., Spors, H., Carleton, A., Margrie, T.W., Kuner, T. and Schaefer, A.T. (2004) Maintaining accuracy at the expense of speed: stimulus similarity defines odor discrimination time in mice. Neuron 44, 865–876.
[85] Rinberg, D., Koulakov, A. and Gelperin, A. (2006) Speed-accuracy tradeoff in olfaction. Neuron 51, 351–358.
[86] Miklavc, P. and Valentinčič, T. (2012) Chemotopy of amino acids on the olfactory bulb predicts olfactory discrimination capabilities of zebrafish Danio rerio. Chem. Senses 37, 65–75.
[87] Olsen, S.R., Bhandawat, V. and Wilson, R.I. (2010) Divisive normalization in olfactory population codes. Neuron 66, 287–299.
[88] Mazor, O. and Laurent, G. (2005) Transient dynamics versus fixed points in odor representations by locust antennal lobe projection neurons. Neuron 48, 661–673.
[89] Isaacson, J.S. (2001) Mechanisms governing dendritic gamma-aminobutyric acid (GABA) release in the rat olfactory bulb. Proc. Natl. Acad. Sci. USA 98, 337–342.
[90] Denk, W., Briggman, K.L. and Helmstaedter, M. (2012) Structural neurobiology: missing link to a mechanistic understanding of neural computation. Nat. Rev. Neurosci. 13, 351–358.
[91] Tabor, R. and Friedrich, R.W. (2008) Pharmacological analysis of ionotropic glutamate receptor function in neuronal circuits of the zebrafish olfactory bulb. PLoS One 3, e1416.